Phonon spectra of diamond and zinc-blende semiconductors

E. O. Kane
Bell Communications Research, Inc., Murray Hill, New Jersey 07974
(Received 14 December 1984)

We model the phonon spectra of the diamond-structure compounds C, Si, Ge, Sn and the zinc-blende-structure compounds GaP, GaAs, and ZnS. We use a four-parameter valence-force model consisting of first- and second-neighbor forces plus the very important coplanar angle-angle interaction introduced by McMurry *et al.* Although formally "fifth neighbor," this interaction follows bond stretching and bond bending in importance. In agreement with the remarkable spread of screening charge along ⟨110⟩ bond chains this interaction highlights the physical importance of these chains. Two-parameter fits to the spectra are quite successful using only bond bending and bond stretching but with much smaller values of bond bending than found by Martin, who fitted the elastic constants. In zinc-blende compounds two bond-stretching parameters are available corresponding to the two distinct vertex atoms. The extra degree of freedom gives little improvement and produces such wildly different values as to call into question the degree of localization implied by the intuitive picture of bond bending. We introduce long-range Coulomb interactions through a "bond-tilt" model yielding dipole-dipole and quadrupole-quadrupole interactions. These interactions further improve the fits given by the valence-force model, yielding an LO-TO splitting for the zinc-blende compounds. The interactions are manifestly rotationally invariant, satisfying a serious question raised by an earlier model due to Lax. Our models give a different perspective on the physics of covalent phonon spectra which we feel is complementary to the bond-charge models of Martin and Weber. The accuracy of our best fits is comparable.

I. INTRODUCTION AND CONCLUSION

The phonon spectra of semiconductors have been extensively studied. A good review and discussion of the physics of covalent phonon spectra is given by Weber.[1] A very comprehensive bibliography of experimental and theoretical phonon spectra of insulators is given by Bilz and Kress.[2] Most of the phonon work has been empirical in nature although, recently, first-principles calculations have also been successful.[3] The latter do not replace the former, however, for many purposes because the physics of the phonon interactions is often revealed more clearly by the empirical models. In addition, applications to problems of lower symmetry, such as the distortion pattern around an impurity, are still too difficult for *a priori* methods and must be treated empirically or, most accurately, by a combination of first-principles calculations of first-neighbor displacement energies coupled with an empirical treatment for more distant neighbors.[4]

Empirical models are vitally concerned with the range of the effective interaction. Early work determined that interactions coupling first and second neighbors were inadequate to describe the pronounced flattening of the TA modes in ⟨100⟩ and ⟨111⟩ directions. It was speculated[5] that long-range forces due to quadrupole-quadrupole interactions might be crucial in obtaining a satisfactory model.

The adiabatic bond-charge model of Martin[6] and Weber[1] introduced long-range Coulomb forces through a specific model based on the physical picture of a bond charge attached by springs to nearest neighbors. It is quite successful in describing the phonon spectra in terms of a small number of parameters.

At about the same time McMurry *et al.*[7] (hereafter MSBN) introduced a valence-force model involving six parameters which gave an equally good fit to diamond and silicon phonon spectra. An important element in their success was the introduction of a fifth-neighbor interaction described in Fig. 1 which we call the MSBN interaction after the authors of Ref. 7. The competition between this model and the bond-charge model then depends in part on the number of parameters involved, six versus four, which tends to favor the bond-charge model by the criterion of simplicity.

We first became involved in this problem through an entirely different approach based on the following idea. The Pauling hybrids on a given atom are mutually orthogonal and complete in the sense that any hybrid in any direction can be described as a linear combination of this set. In a sense then, the usual interpretation of the bond-bending interaction is misleading since it implies that the bond remains straight and the angle between bonds changes. A better picture might be that of tetrahedrally oriented hybrids on each atom which are rigid but free to rotate. The distortion energy would then be proportional to the square of the deviation from colinearity of the two hybrids making up a bond. Unfortunately, this description was more difficult to implement than the conventional one and did not lead to superior results so it was abandoned. The possibility remains, however, that the charge distribution is more correctly described in this model.

Recently we discovered[8] that the charge disturbance due to an impurity at the origin in the diamond lattice spreads with striking directionality along coplanar chains of bonds. This observation provides a rationale for the importance of the MSBN interaction which consists of

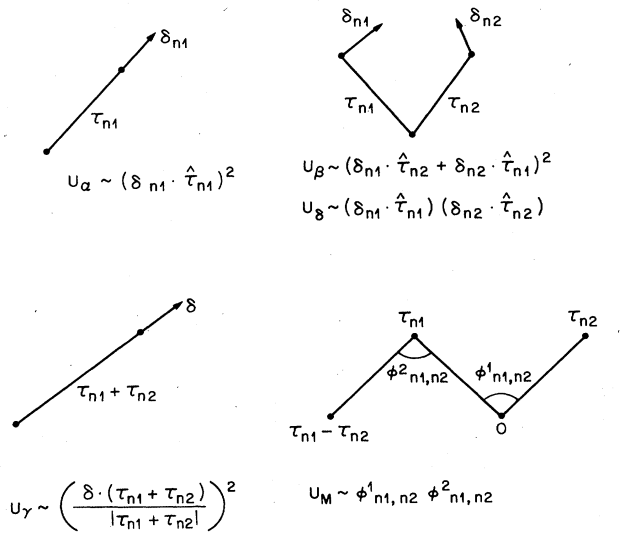

FIG. 1. Interactions U_α, U_β, U_γ, U_δ, and U_M defined in Eqs. (6), (8), (11), (14), and (16) are depicted graphically. U_α is bond stretching, U_β is Keating's bond-bending interaction, U_δ is contiguous bond stretching, U_γ is second-neighbor stretching, and U_M is the MSBN interaction introduced in Ref. 7. The angles ϕ^1,ϕ^2 in U_M are coplanar in the (110) plane.

the product of consecutive angles along a coplanar chain. (See Fig. 1.) Instead of being considered merely as a "fifth-neighbor" interaction, it appears as one of the most likely candidates to consider after all second-neighbor interactions are investigated. With this perspective we have reanalyzed the valence-force model and considered only the four independent first- and second-neighbor interactions plus the MSBN interaction.

We follow the most common convention in defining our interactions to be bond stretching, bond bending, second-neighbor "bond" stretching, fourth degree of freedom, MSBN interaction, or $U_\alpha, U_\beta, U_\gamma, U_\delta, U_M$. See the mathematical description in Sec. II. With $U_\alpha, U_\beta, U_\gamma$ defined, all choices for the fourth degree of freedom are equivalent. We have then ordered the interactions according to successively optimal 1-, 2-, 3-, 4-, 5-parameter fits to the experimental phonons. The ordered sequence is $U_\alpha, U_\beta, U_M, U_\gamma, U_\delta$. U_δ gives only a slight improvement to the fit, hence it may be said that a satisfactory valence-force model can be defined in terms of only four interactions without any long-range Coulomb interactions. For many applications it is very convenient not to have to consider Coulomb interactions.

A further point in favor of our model is that the bond-charge model requires five parameters to fit diamond which for us is not a special case. The relative accuracy of the two four-parameter descriptions is not easy to assess without using the same fitting procedures for both models. The two are comparable. Ours appears to be less accurate but easier to implement. In terms of physics, the two models are complementary. Our model focuses attention on the MSBN interaction whereas Weber's model focuses on the bond charge.

Our model can be further improved by adding dipole-dipole and quadrupole-quadrupole interactions in the spirit of Lax's original suggestion.[5] Every bond possesses a dipole and a quadrupole moment in the perfect crystal. A distortion of the crystal may lead to a change in this moment proportional to the stretching or the tilting of the bonds. Formulated in this way, our interactions are manifestly rotationally invariant, which we believe is not true of Lax's original model.

We find that the bond-tilt model gives a better fit than bond stretching. Furthermore, the multipole interactions can be modified by a smearing of the **r**-space interaction which leads to better convergence in **k** space. In addition to the computational convenience, the smearing also improves the fits. The importance of the quadrupole-quadrupole interaction increases monotonically from diamond to tin.

We have also used our bond model for the dipole moment together with the valence-force interactions $U_\alpha, U_\beta, U_\gamma, U_M$ to fit the phonon spectra of the zinc-blende-structure compounds GaAs, GaP, and ZnS. The interactions U_β, U_γ are different in the zinc-blende lattice depending on the vertex atom, leading to a total of six interaction parameters. (The dipole-dipole interaction is fixed to give the correct LO-TO splitting at $k=0$.) The fits are slightly less good and the number of parameters is greater than the fits to the diamond-lattice phonons. We also give two parameter fits to the spectra for $U_\alpha, U_{\beta 1} = U_{\beta 2}$. The magnitudes of the fitting coefficients β_1, β_2 have the opposite sign and are much larger when allowed to differ than when constrained to be equal.

Our two-parameter fits for both diamond and zinc-blende materials are quite different from Martin's[9] results who fitted bond stretching and bending to the elastic constants. Our values of bond bending are significantly lower than Martin's because of the strong flattening of the TA phonons away from the origin. For applications such as calculating the distortion pattern around an impurity our numbers are to be preferred because the low Fourier components of the distortion pattern have little weight.

In Sec. II we describe the models that we use for the phonon energies including the valence-force models (Sec. II B) and the Coulomb interactions (Sec. II C). In Sec. II D we describe our empirical models for obtaining the phonon-induced multipole moments. In Sec. II E we describe the Ewald method used to perform the multipole lattice sums. In Sec. II F we discuss the LO-TO splitting of the ionic compounds.

In Sec. III we describe our empirical parameter fitting techniques and give some detailed discussion of the individual parameter values. Tables and graphs of the fitting functions are presented.

II. PHONON ENERGY CALCULATIONS

A. Dynamical matrix

For a given phonon **k** there are six independent degrees of freedom corresponding to the two vector displacements $\mathbf{r}(\mathbf{0})$, $\mathbf{r}(\tau_1)$. All other displacements $\mathbf{r}(\mathbf{a}_l), \mathbf{r}(\tau_1+\mathbf{a}_l)$ are related to these by the phase factor $\exp(i\mathbf{k}\cdot\mathbf{a}_l)$.

We write the potential energy in the form

$$U=\sum_{i,j=1}^{3}\sum_{t_1t_2=0,\tau_1}\sum_{a_l,a_{d1},a_{d2}} u_{ij}(t_1+a_{d1},t_2+a_{d2})r_i(t_1+a_{d1}+a_l)r_j(t_2+a_{d2}+a_l)\ . \tag{1}$$

a_l are vectors belonging to the fcc lattice; and a_{d1},a_{d2} are members of a subset of fcc. $0,\tau_1$ are the basis vectors of the diamond lattice. It is easy to show that the dynamical matrix can be written[10]

$$\begin{aligned}
&D_{ij}(t_1,t_2)=\frac{\partial^2U^*}{\partial r_i^*(t_1)\partial r_j(t_2)}\frac{1}{[M_A(t_1)M_A(t_2)]^{1/2}}\\
&U^*=\sum_{\substack{i,j,t_1,t_2,\\ a_{d1},a_{d2}}} U_{ij}(t_1+a_{d1},t_2+a_{d2})\\
&\qquad\times[r_i^*(t_1+a_{d1})r_j(t_2+a_{d2})\\
&\qquad\qquad +r_i(t_1+a_{d1})r_j^*(t_2+a_{d2})]\ ,\\
&r_i(t+a_d)=e^{ik\cdot a_d}r_i(t)\ ,\\
&r_i^*(t+a_d)=e^{-ik\cdot a_d}r_i^*(t)\ .
\end{aligned} \tag{2}$$

In Eq. (2) r_i^* and r_i are to be treated as independent variables. Use has been made of the relations

$$\begin{aligned}
&r_i(t_1+a_l)=e^{ik\cdot a_l}r_i(t_1)\ ,\\
&U_{ij}(t_1+a_{d1}+a_l,t_2+a_{d2}+a_l)=U_{ij}(t_1+a_{d1},t_2+a_{d2})\ ,
\end{aligned} \tag{2a}$$

which follow from translational invariance.

The eigenvalues of the 6×6 dynamical matrix give ω^2, where $\omega=2\pi\nu$ and ν is the phonon frequency.

B. Valence-force model

We follow Keating's[11] model in defining the bond-stretching and bond-bending interactions U_α and U_β, but we expand his expressions to keep only quadratic terms. The higher-order terms lead to anharmonic effects which have not been shown to be satisfactorily treated by this model. We then find for bond stretching

$$U_\alpha=\tfrac{3}{2}\sum_{\substack{n=1,4\\ a_l=\text{fcc}}}^{4}(\delta b_{n,l})^2\ , \tag{3}$$

$$\delta\mathbf{b}_{n,l}=\mathbf{r}(\tau_n+\mathbf{a}_l)-\mathbf{r}(\mathbf{a}_l)\ , \tag{4}$$

$$\delta b_{n,l}=\delta\mathbf{b}_{n,l}\cdot\hat{\tau}_n\ , \tag{5}$$

$$\tau_n=\mathbf{n}_n a_L/4=\hat{\tau}_n\tau\ , \tag{6}$$

$$\hat{\tau}_n=\mathbf{n}_n/\sqrt{3}\ ,\quad \mathbf{n}_1=(1,1,1),\ \mathbf{n}_2=(1,-1,-1)\ ,\quad \mathbf{n}_3=(-1,1,-1),\ \mathbf{n}_4=(-1,-1,1)\ . \tag{7}$$

Bond bending is given by

$$U_{\beta m}=\tfrac{3}{8}\sum_{\substack{n_1,n_2=1\\ n_1>n_2\\ a_l=\text{fcc}}}^{4}(\beta_{n_1,n_2}^{m,l}+\beta_{n_2,n_1}^{m,l})^2,\quad m=0,1 \tag{8}$$

$$\beta_{n_1,n_2}^{0,l}=[\mathbf{r}(\tau_{n_1}+\mathbf{a}_l)-\mathbf{r}(\mathbf{a}_l)]\cdot\hat{\tau}_{n_2}\ , \tag{9}$$

$$\beta_{n_1,n_2}^{1,l}=[\mathbf{r}(\tau_1+\mathbf{a}_l)-\mathbf{r}(\tau_1-\tau_{n_1}+\mathbf{a}_l)]\cdot\hat{\tau}_{n_2}\ . \tag{10}$$

We define second-neighbor "bond stretching" in a manner completely analogous to Eq. (3):

$$U_{\gamma m}=\tfrac{3}{2}\sum_{\substack{n=1\\ a_l=\text{fcc}}}^{12}(\delta c_n^{ml})^2,\quad m=0,1\ , \tag{11}$$

$$\begin{aligned}
&\delta\mathbf{c}_n^{0,l}=\mathbf{r}(\mathbf{a}_n+\mathbf{a}_l)-r(\mathbf{a}_l)\ ,\\
&\delta\mathbf{c}_n^{1,l}=\mathbf{r}(\mathbf{a}_n+\tau_1+\mathbf{a}_l)-\mathbf{r}(\tau_1+\mathbf{a}_l)\ ,\\
&\mathbf{a}_1=(0,1,1)a_L/2,\ \text{etc.}\ ,
\end{aligned} \tag{12}$$

$$\delta c_n^{m,l}=\delta\mathbf{c}_n^{m,l}\cdot\hat{\mathbf{a}}_n\ , \tag{13}$$

where $\hat{\mathbf{a}}_n$ is a unit vector in the direction of $\mathbf{a}_n$.

For the final valence-force interaction between second neighbors we choose the following:

$$U_{\delta m}=\sum_{\substack{n_1>n_2\\ a_l=\text{fcc}}}\delta b_{n_1}^{m,l}\delta b_{n_2}^{m,l},\quad m=0,1 \tag{14}$$

where

$$\begin{aligned}
&\delta\mathbf{b}_n^{0,l}=\mathbf{r}(\tau_n+\mathbf{a}_l)-\mathbf{r}(\mathbf{a}_l)\ ,\\
&\delta\mathbf{b}_n^{1,l}=\mathbf{r}(\tau_1+\mathbf{a}_l)-\mathbf{r}(\tau_1-\tau_n+\mathbf{a}_l)\ ,\\
&\delta b_n^{m,l}=\delta\mathbf{b}_n^{m,l}\cdot\hat{\tau}_n\ ,
\end{aligned} \tag{15}$$

in complete analogy to Eqs. (4) and (5).

We define the MSBN interaction[7] according to

$$U_M=\tau^2\sum_{\substack{n_1,n_2=1,4\\ n_1\neq n_2\\ a_l=\text{fcc}}}\delta\phi_{n_1,n_2}^{0,l}\delta\phi_{n_1,n_2}^{n_1,l}\ , \tag{16}$$

$$\begin{aligned}
\delta\phi_{n_1,n_2}^{m,l}=-\frac{1}{\tau\sin\phi_0}[&\delta\mathbf{b}_{n_1}^{m,l}\cdot(\hat{\tau}_{n_2}+\tfrac{1}{3}\hat{\tau}_{n_1})\\
&+\delta\mathbf{b}_{n_2}^{m,l}\cdot(\hat{\tau}_{n_1}+\tfrac{1}{3}\hat{\tau}_{n_2})],\quad m=0,n_1
\end{aligned} \tag{17}$$

$$\delta\mathbf{b}_{n_2}^{n_1,l}=\mathbf{r}(\tau_{n_1}+\mathbf{a}_l)-\mathbf{r}(\tau_{n_1}-\tau_{n_2}+\mathbf{a}_l),\quad \sin^2\phi_0=\tfrac{8}{9}\ . \tag{18}$$

The seven interactions $U_\alpha,U_{\beta0},U_{\beta1},U_{\gamma0},U_{\gamma1},U_{\delta0},U_{\delta1}$ constitute all the independent valence-force interactions between first and second neighbors in the zinc-blende lattice. In the diamond lattice $U_{\beta0}=U_{\beta1}$, $U_{\gamma0}=U_{\gamma1}$, and $U_{\delta0}=U_{\delta1}$.

C. Coulomb-interaction moment expansion

We write the Coulomb interaction between two charges e_a and e_b as

$$E = e_a e_b / |\mathbf{R}_a + \boldsymbol{\sigma}_a - \mathbf{R}_b - \boldsymbol{\sigma}_b| \ , \tag{19}$$

where $\boldsymbol{\sigma}_a, \boldsymbol{\sigma}_b$ are the locations of e_a, e_b referred to their respective lattice sites, $\mathbf{R}_a$ and $\mathbf{R}_b$.

We then expand Eq. (19) in a Taylor series in $\boldsymbol{\sigma}_a - \boldsymbol{\sigma}_b$ to fourth order, assuming $\mathbf{R}_a \neq \mathbf{R}_b$. We thus obtain

$$\begin{aligned}
&E = E^0 + E^1 + E^2 + E^3 + E^4 \ , \\
&E^0 = V^0 M_a^0 M_b^0 \ , \\
&E^1 = \sum_i F_i^1 (M_{ai}^1 M_b^0 + M_a^0 M_{bi}^1) \ , \\
&E^2 = \tfrac{1}{2} \sum_{i,j} F_{ij}^2 (M_{aij}^2 M_b^0 + M_a^0 M_{bij}^2 - 2 M_{ai}^1 M_{bj}^1) \ , \\
&E^3 = \tfrac{1}{6} \sum_{i,j,k} F_{ijk}^3 (M_{aijk}^3 M_b^0 - M_{bijk}^3 M_a^0 \\
&\qquad - 3 M_{aij}^2 M_{bk}^1 + 3 M_{ai}^1 M_{bjk}^2) \ , \\
&E^4 = \tfrac{1}{24} \sum_{i,j,k,l} F_{ijkl}^4 (M_{aijkl}^4 M_b^0 + M_a^0 M_{bijkl}^4 - 4 M_{aijk}^3 M_{bl}^1 \\
&\qquad - 4 M_{ai}^1 M_{bjkl}^3 + 6 M_{aij}^2 M_{bkl}^2) \ ,
\end{aligned} \tag{20}$$

$$\begin{aligned}
&F_i^1 = x_i V^1 \ , \\
&F_{ij}^2 = x_i x_j (V^2 - V^1/r) + \delta_{ij} V^1 r \ , \\
&F_{ijk}^3 = x_i x_j x_k \left[V^3 - \frac{3V^2}{r} + \frac{3V^1}{r^2} \right] \\
&\qquad + (\delta_{ik} x_j + \delta_{jk} x_i + \delta_{ij} x_k) \left[\frac{V^2}{r} - \frac{V^1}{r^2} \right] \ , \\
&F_{ijkl}^4 = x_i x_j x_k x_l \left[V^4 - \frac{6V^3}{r} + \frac{15V^2}{r^2} - \frac{15V}{r^3} \right] \\
&\qquad + (\delta_{li} x_j x_k + \delta_{lj} x_i x_k + \delta_{lk} x_i x_j + \delta_{ik} x_j x_l + \delta_{jk} x_i x_l \\
&\qquad + \delta_{ij} x_k x_l) \left[\frac{V^3}{r} - \frac{3V^2}{r^2} + \frac{3V^1}{r^5} \right] \\
&\qquad + (\delta_{ik}\delta_{jl} + \delta_{jk}\delta_{il} + \delta_{ij}\delta_{kl}) \left[\frac{V^2}{r^2} - \frac{V^1}{r^3} \right] \ ,
\end{aligned} \tag{21}$$

$$X_i = (R_{ai} - R_{bi}), \quad r^2 = X_1^2 + X_2^2 + X_3^2, \quad x_i = X_i / r \ , \tag{22}$$

$$V^n = d^n V(r) / dr^n \ , \tag{23}$$

$$\begin{aligned}
&M_a^0 = e_a, \quad M_{ai}^1 = e_a \sigma_{ai}, \quad M_{aij}^2 = e_a \sigma_{ai} \sigma_{aj} \ , \\
&M_{aijk}^3 = e_a \sigma_{ai} \sigma_{aj} \sigma_{ak}, \quad M_{aijkl}^4 = e_a \sigma_{ai} \sigma_{aj} \sigma_{ak} \sigma_{al} \ .
\end{aligned} \tag{24}$$

Then, in order to obtain the total Coulomb energy of the charge distribution, we sum over all the charge pertaining to sites $\mathbf{R}_a$ and $\mathbf{R}_b$. Equations (24) then give the monopole, dipole, quadrupole, and octupole moments. M^2 can be taken to be a traceless tensor since the trace does not contribute to the Coulomb interaction. $V(r) = 1/r$, but more general forms will be used later in the Ewald transformation.

We also sum over all pairs of lattice sites $\mathbf{R}_a, \mathbf{R}_b$ to give the total energy. We ignore M^0, M^3, M^4. The total energies E^2, E^4 become

$$\begin{aligned}
&E^2 = - \sum_{\substack{i,j,\mathbf{R}_a,\mathbf{R}_b \\ \mathbf{R}_a \neq \mathbf{R}_b}} F_{ij}^2 (\mathbf{R}_a - \mathbf{R}_b) M_i^1 (\mathbf{R}_a) M_j^1 (\mathbf{R}_b) \ , \\
&E^4 = \tfrac{1}{4} \sum_{\substack{i,j,k,l,\mathbf{R}_a,\mathbf{R}_b \\ \mathbf{R}_a \neq \mathbf{R}_b}} F_{ijkl}^4 M_{ij}^2 (\mathbf{R}_a) M_{kl}^2 (\mathbf{R}_b) \ .
\end{aligned} \tag{24a}$$

Then writing

$$\mathbf{R}_a = \mathbf{t}_a + \mathbf{a}_l + \mathbf{a}_d, \quad \mathbf{R}_b = \mathbf{t}_b + \mathbf{a}_l \tag{24b}$$

and using Eqs. (1) and (2), we obtain the form E^{2*} yielding the dynamical matrix

$$\begin{aligned}
E^{2*} = - \sum_{\substack{i,j=1 \\ \mathbf{t}_a, \mathbf{t}_b = 0, \tau_1 \\ \mathbf{a}_d = \text{fcc}}}^{3} & F_{ij}^2 (\mathbf{t}_a - \mathbf{t}_b + \mathbf{a}_d) \\
& \times \{ M_i^1 (\mathbf{t}_a) [M_j^1 (\mathbf{t}_b)]^* e^{i\mathbf{k}\cdot\mathbf{a}_d} \\
& + [M_i^1 (\mathbf{t}_a)]^* M_j^1 (\mathbf{t}_b) e^{-i\mathbf{k}\cdot\mathbf{a}_d} \} \ ,
\end{aligned} \tag{24c}$$

which can be simplified to

$$E^{2*} = -2 \sum_{\substack{i,j \\ \mathbf{t}_a \mathbf{t}_b = 0, \tau_1}} G_{ij}^2 (\mathbf{t}_a - \mathbf{t}_b) M_i^1 (\mathbf{t}_a) [M_j^1 (\mathbf{t}_b)]^* \ , \tag{24d}$$

$$G_{ij}^2 (\mathbf{t}_a - \mathbf{t}_b) = \sum_{\mathbf{a}_d = \text{fcc}} F_{ij}^2 (\mathbf{t}_a - \mathbf{t}_b + \mathbf{a}_d) e^{i\mathbf{k}\cdot\mathbf{a}_d} \ . \tag{24e}$$

Similarly we find

$$\begin{aligned}
E^{3*} = \sum_{\substack{i,j,k=1, \\ \mathbf{t}_a \mathbf{t}_b = 0, \tau_1}}^{3} & G_{ijk}^2 (\mathbf{t}_a - \mathbf{t}_b) [- M_{ij}^2 (\mathbf{t}_a) M_k^2 (\mathbf{t}_b)^* \\
& + M_i^1 (\mathbf{t}_a) M_{jk}^2 (\mathbf{t}_b)^*] \ ,
\end{aligned} \tag{24f}$$

$$\begin{aligned}
&E^{4*} = \tfrac{1}{2} \sum_{\substack{i,j,k,l=1 \\ \mathbf{t}_a \mathbf{t}_b = 0, \tau_1}}^{3} G_{ijkl}^4 (\mathbf{t}_a - \mathbf{t}_b) M_{ij}^2 (\mathbf{t}_a) M_{kl}^2 (\mathbf{t}_b)^* \ , \\
&G_{ijk}^3 (\mathbf{t}_a - \mathbf{t}_b) = \sum_{\mathbf{a}_d = \text{fcc}} F_{ijk}^3 (\mathbf{t}_a - \mathbf{t}_b + \mathbf{a}_d) e^{i\mathbf{k}\cdot\mathbf{a}_d} \ , \\
&G_{ijkl}^4 (\mathbf{t}_a - \mathbf{t}_b) = \sum_{\mathbf{a}_d = \text{fcc}} F_{ijkl}^4 (\mathbf{t}_a - \mathbf{t}_b + \mathbf{a}_d) e^{i\mathbf{k}\cdot\mathbf{a}_d} \ .
\end{aligned} \tag{24g}$$

D. Empirical multipole models

We need to calculate the multipole moments of Eq. (24) in the presence of a phonon distortion. It is now possible

to do such calculations by *a priori* methods[3] but we will introduce an empirical model which ignores multipoles higher than quadrupole.

In the undistorted lattice there are no dipole or quadrupole moments. There are monopole moments in zinc blende but not in diamond. The phonon interaction is quadratic and we assume that the individual moments M_a, M_b are separately linear. (A quadratic multipole combined with a monopole seems possible in zinc blende but we ignore this possibility.)

The simplest model for the zinc-blende lattice, following Kellermann,[12] is to assume that the phonons rigidly displace the lattice charge distribution

$$\sigma_{ai} = \sigma^0_{ai} + r_i(\mathbf{R}_a) , \tag{25}$$

where $r_i(\mathbf{R}_a)$ is the phonon displacement of lattice site, $\mathbf{R}_a$. This leads to dipole moments of the form

$$M^1_{ai} = M^0_a r_i(\mathbf{R}_a) . \tag{26}$$

Substitution of (25) in M^2_a, M^3_a in Eqs. (24a)—(24g) gives zero to first order in r since M^1_a, M^2_a are zero in the perfect lattice. M^0_a is a property of the undistorted lattice in this model but we use it as an empirical constant. Charge neutrality requires $M^0_\tau = -M^0_0$.

III. BOND-STRETCH AND BOND-TILT MULTIPOLES

We now proceed to develop two phenomenological models for the dipole and quadrupole moments in the diamond or zinc-blende lattices. We imagine that all of the valence charge has been assigned to the four bonds around each atom and that the charge in each bond has been divided between the two atoms forming the bond. In the diamond lattice a logical choice would be to assign the charge to the closer of the two atoms. We then expand the charge in monopole, dipole, and quadrupole moments about each lattice site.

For the unperturbed bond dipoles we write

$$\mathbf{d}^a_n = D^0(a)\hat{\tau}_n , \tag{27}$$

where $\mathbf{d}^a_n$ is the dipole moment at lattice site $\mathbf{R}_a$ associated with bond $n = 1,4$ and $\hat{\tau}_n$ is a unit bond vector defined as in Eqs. (6) and (7). The phenomenological constant $D^0(a)$ depends on whether $\mathbf{R}_a$ is on the $\mathbf{R}_a = \mathbf{0}$ or $\mathbf{R}_a = \tau_1$ sublattice. In the diamond lattice $D^0(\tau_1) = -D^0(\mathbf{0})$.

In the "bond-stretch" model we assume that the dipoles in the distorted lattice are proportional to the bond lengths. The dipole-moment change is then given by

$$\delta\mathbf{d}^a_n = D^s(a)\hat{\tau}_n \, \delta b^a_n / \tau \quad \text{(bond stretch)} . \tag{28}$$

TABLE I. Diamond. Fits to the experimental phonon spectrum of diamond with varying numbers of fitting parameters. Columns 1 and 2 give the **k** vectors and frequencies of the experimental phonons. Column 3 gives the weights used in the least-squares fitting including the degeneracy of the level. The remaining columns give the errors in the fits, experiment − theory, for increasing numbers of parameters δ_n. The maximum percentage error (Max % error) of the fit is also given. The difference with the largest percent error in each column is indicated by an asterisk. The parameter values corresponding to column δ_n are given in row n below in units 10^3 ergs/cm^2.

k (units of $2\pi/a_L$)	ν (10^{12} Hz)	Weight	δ_1	δ_2	δ_3	δ_4
(0.4,0,0)	13.66	10	1.53*	0.86*	0.52	0.17
	37.73	2	−1.67	0.43	−0.21	0.13
(1,0,0)	24.09	10	−0.45	−0.42	0.09	0.11
	32.32	2	−0.81	−1.07	1.03	0.67
	35.82	2	1.90	0.91	−0.93	−0.16
(0.5,0.5,0.5)	16.56	10	−0.79	−0.77	−0.41	−0.40
	31.04	1	1.07	−1.34	−0.38	−0.21
	36.30	2	−1.10	0.34	0.10	0.19
	37.25	1	1.86	1.62	−0.23	0.48
(0.0,0.6,0.6)	20.86	10	1.00	1.03	0.15	0.04
	25.79	2	−0.34	−1.26	−1.42*	−1.00*
	27.70	2	1.27	−0.29	−0.02	0.78
	34.23	2				0.26
	37.25	2				−0.69
Max % error			11	6.3	5.5	4

n	α	β	γ	μ	δ
1	108.13	59.24	0.0	0.0	0.0
2	98.83	47.53	3.83	0.0	0.0
3	80.50	40.81	5.29	7.56	0.0
4	67.23	35.97	6.87	8.26	−16.15

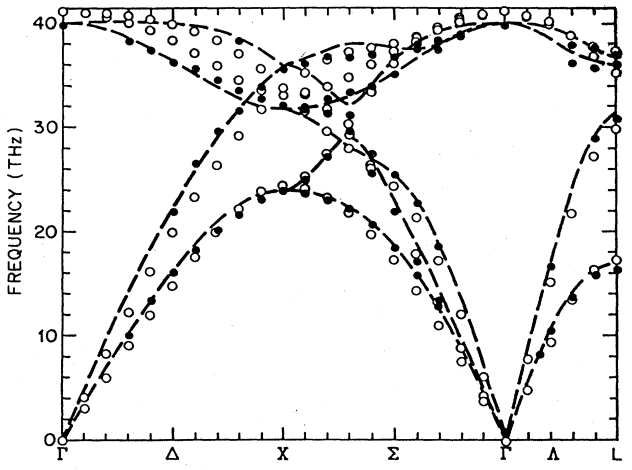

FIG. 2. Phonon dispersion curves for diamond. The open circles and dashes correspond to fits δ_1 and δ_4 in Table I. The solid circles are experimental data from Ref. 14.

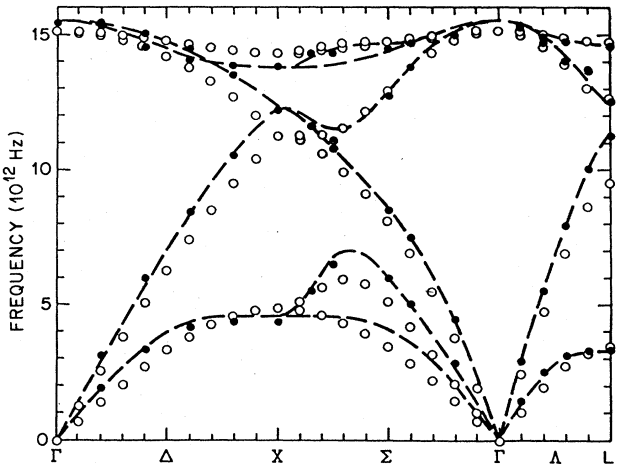

FIG. 3. Phonon dispersion curves for silicon. The open circles and dashes correspond to fits δ_1 and δ_5 in Table II. The solid circles are experimental data from Refs. 15 and 16.

The change in bond length δb_n^a is given by Eq. (15) if we identify $a=0$ and $a=\tau$ with 0 and 1. $D^s(a)$ is a new phenomenological constant analogous to $D^0(a)$.

In the "bond-tilt" model we assume that the bond dipole moment follows the unit vector $\hat{\mathbf{b}}_n^a$ defined by

$$\hat{\mathbf{b}}_n^a=\hat{\tau}_n+[\delta\mathbf{b}_n^a-(\delta\mathbf{b}_n^a\cdot\hat{\tau}_n)\hat{\tau}_n]/\tau \tag{29}$$

using definitions in Eqs. (15). The dipole moment change is then found by substituting $\hat{\mathbf{b}}_n^a$ for $\hat{\tau}_n$ in Eq. (27):

$$\delta\mathbf{d}_n^a=D^0(a)[\delta\mathbf{b}_n^a-(\delta\mathbf{b}_n^a\cdot\hat{\tau}_n)\hat{\tau}_n]/\tau \quad \text{(bond tilt)} . \tag{30}$$

TABLE II. Silicon. See Table I.

k (units of $2\pi/a_L$)	ν (10^{12} Hz)	Weight	δ_1	δ_2	δ_3	δ_4	δ_5
(0.4,0,0)	3.47	10	0.69*	0.17	−0.03	0.08	0.02
	6.10	1	0.98	0.65*	0.17	0.03	0.32*
	14.65	2	−0.30	−0.47	−0.10	−0.11	−0.14
	15.15	1	0.55	−0.12	0.18	0.08	0.12
(1,0,0)	4.51	10	−0.41	−0.08	−0.04	−0.06	−0.04
	12.32	2	1.0	0.56	0.08	−0.15	0.03
	13.90	2	−0.49	0.20	−0.03	0.12	0.19
(0.5,0.5,0.5)	3.41	10	−0.07	0.17	0.20	0.18	0.10
	11.35	1	1.8	1.12	0.90*	0.64*	0.07
	12.60	1	0.02	0.62	−0.19	0.21	0.24
	14.68	2	−0.12	−0.21	−0.01	0.03	0.07
(0,0.7,0.7)	4.54	10	0.16	−0.04	−0.05	−0.02	0.03
	6.76	2	0.75	−0.26	−0.34	−0.24	−0.18
(0,0.75,0.75)	10.85	2					0.11
	11.15	2					−0.32
	14.40	2					−0.03
Max % error			20	11	8	6	5

n	α	β	γ	μ	δ	c_4
1	47.64	5.56	0	0	0	0
2	43.23	4.84	0	2.03	0	0
3	41.47	1.58	1.06	2.19	0	0
4	44.46	2.75	0.68	1.99	4.18	0
5	41.31	2.74	0.64	1.91	0	0.001 33

In the undistorted lattice the sum over all four bonds must lead to zero net dipole and quadrupole moments by symmetry.

For the unperturbed bond quadrupoles we write

$$q_{ij}^{a,n}=Q^0(a)(\tfrac{3}{2}\hat{\tau}_{ni}\hat{\tau}_{nj}-\tfrac{1}{2}\delta_{ij}) , \tag{31}$$

which is a symmetric traceless tensor with an axis of rotation in the direction $\hat{\tau}_n$. In the diamond lattice the empirical constants satisfy the symmetry relation $Q^0(\tau_1)=Q^0(\mathbf{0})$.

We proceed to define stretch and tilt quadrupole moments in complete analogy to the dipole definitions.

$$\delta q_{ij}^{a,n}=Q^s(a)(\tfrac{3}{2}\hat{\tau}_{ni}\hat{\tau}_{nj}-\tfrac{1}{2}\delta_{ij})\delta b_n^a/\tau \quad \text{(bond stretch)} ,$$
$$\delta q_{ij}^{a,n}=\tfrac{3}{2}Q^0(a)(\hat{\tau}_{ni}\delta\hat{b}_{nj}^{\,a}+\hat{\tau}_{nj}\delta\hat{b}_{ni}^{\,a}) \quad \text{(bond tilt)} . \tag{32}$$

The total dipole and quadrupole moment at the site a is obtained, of course, by summing Eqs. (28), (30), and (32) over all bonds $n=1,4$.

A. Ewald method

The quantities G^2,G^3,G^4 in Eqs. (24e) and (24g) involve sums over all fcc Bravais lattice points. We calculate these sums using an Ewald method.[12] We divide the Coulomb interaction in two sections:

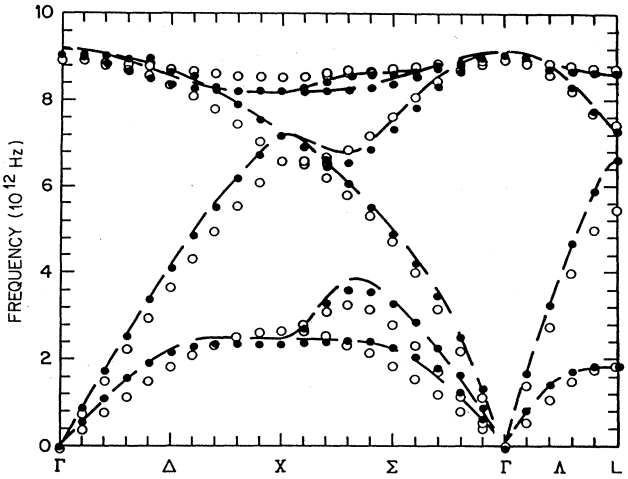

FIG. 4. Phonon dispersion curves for germanium. Open circles and dashes correspond to fits δ_1 and δ_5 in Table III. The solid circles are experimental data from Refs. 17 and 18.

$$1/r=F_q(r)+F_\rho(r) ,$$
$$F_q(r)=(1/r)\mathrm{erf}(fr) . \tag{33}$$

$F_q(r)$ is Fourier analyzed and summed in $\mathbf{k}$ space, $F_\rho(r)$ is

TABLE III. Germanium. See Table I.

$\mathbf{k}$ (units of $2\pi/a_L$)	ν (10^{12} Hz)	Weight	δ_1	δ_2	δ_3	δ_4	δ_5
(0.4,0,0)	1.96	10	0.43*	0.09	−0.02	0.04	0.01
	3.42	1	0.43	0.24	−0.03	−0.06	0.06
	8.56	2	−0.28	−0.38	−0.13	−0.15	−0.18
	8.95	1	−0.35	−0.05	0.16	0.10	0.10
(1,0,0)	2.40	10	−0.29	−0.07	−0.04	−0.05	−0.05
	7.21	2	0.59	0.31	0.06	0.001	0.008
	8.26	2	−0.30	0.10	0.01	0.10	0.12
(0.5,0.5,0.5)	1.90	10	0.002	0.15	0.17	0.17*	0.10*
	6.66	1	1.18	0.77*	0.66*	0.56	0.019
	7.34	1	−0.13	0.22	−0.21	−0.16	0.03
	8.70	2	−0.07	−0.12	0.03	0.05	0.07
(0,0.7,0.7)	2.49	10	0.10	−0.03	−0.03	−0.02	0.04
	3.66	2	0.38	−0.27	−0.30	−0.25	−0.17*
	6.10	2	0.26	0.26	0.01	−0.09	0.04
	6.58	2					−0.19
	8.29	2					0.02
	8.63	2					0.04
Max % error			22	12	10	9	5

n	α	β	γ	μ	δ	c_4
1	43.56	4.29	0	0	0	0
2	39.64	3.63	0	1.80	0	0
3	37.73	0.80	0.91	1.96	0	0
4	39.69	1.87	0.57	1.83	2.74	0
5	37.87	1.88	0.52	1.63	0	0.001 49

summed in r space. The Ewald parameter, f, is selected to optimize convergence.

Taking the Fourier transform of $F_q(r)$,

$$\tilde{F}_q(\mathbf{k})=\frac{4\pi}{k^2}\exp(-k^2/4f^2)\ , \tag{34}$$

we obtain the lattice sum

$$\sum_{\mathbf{a}_l} F_q(\mathbf{a}_l+\mathbf{r})e^{i\mathbf{k}\cdot\mathbf{a}_l}=\frac{N}{\text{vol}}\sum_{\mathbf{K}}\tilde{F}_q(\mathbf{K}-\mathbf{k})e^{i(\mathbf{K}-\mathbf{k})\cdot\mathbf{r}}+C(\mathbf{r})\ , \tag{35}$$

$$C(\tau_1)=0;\quad C(\mathbf{0})\equiv\lim_{\mathbf{r}\to 0}-F_q(\mathbf{r})\ . \tag{36}$$

The correction term compensates for the fact that the lattice site $\mathbf{a}_l=\mathbf{0}$ is omitted on the left-hand side of Eq. (35) when $\mathbf{r}=\mathbf{0}$. We can then differentiate both sides of Eq. (35) with respect to $\mathbf{r}$ two, three, or four times to obtain G^2,G^3,G^4 in Eqs. (24e) and (24g).

The contribution to G^2,G^3,G^4 from $F_\rho(r)$ in Eq. (33) is evaluated directly in $\mathbf{r}$ space. The contribution from $F_q(r)$ is evaluated in $\mathbf{k}$ space using the right-hand side of Eq. (35) after differentiation. The result should be independent of f in Eq. (33) which provides a very good check.

In the diamond lattice the condition $D(\tau_1)=-D(\mathbf{0})$ for the dipole moments leads to an approximate cancellation at large distance. In fact, the two dipoles cancel to the extent that they become equivalent to a quadrupole at $\tau/2$. Hence, the long-range Coulomb interactions are phenomenologically the same in either dipole or quadrupole models. In the zinc-blende lattice there is no relation between $D(\tau_1)$ and $D(\mathbf{0})$. We may break down the parameters into two terms D_+ and D_-:

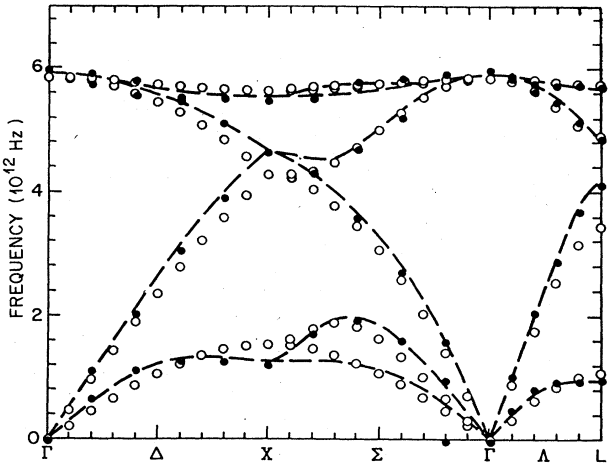

FIG. 5. Phonon dispersion curves for grey tin. Open circles and dashes correspond to fits δ_1 and δ_5 in Table IV. Solid circles are experimental data from Ref. 19.

TABLE IV. Grey tin. See Table I.

$\mathbf{k}$ (units of $2\pi/a_L$)	ν (10^{12} Hz)	Weight	δ_1	δ_2	δ_3	δ_4	δ_5
(0.4,0,0)	1.15	10	0.26	0.15	0.11	0.14*	0.074*
	2.05	1	0.13	0.07	−0.09	−0.14	−0.08
	5.61	2	−0.19	−0.23	−0.09	−0.11	−0.12
	5.82	1	0.20	0.06	0.19	0.11	0.12
(1,0,0)	1.25	10	−0.30*	−0.04	−0.02	−0.03	−0.010
	4.67	2	0.38	0.30	0.16	0.07	0.02
	5.51	2	−0.15	−0.02	−0.09	0.02	−0.02
(0.5,0.5,0.5)	1.00	10	−0.10	0.09	0.11	0.10	0.04
	4.15	1	0.70	0.62*	0.56*	0.42	−0.05
	4.89	1	−0.04	0.08	−0.18	−0.11	−0.05
	5.74	2	−0.02	−0.06	0.03	0.04	0.05
(0,0.6,0.6)	1.96	10	0.12	−0.04	−0.04	−0.03	−0.009
	3.61	2	0.14	0.18	0.03	−0.09	−0.03
	4.73	2					−0.01
	5.78	2					0.03
Max % error			24	15	13.5	12	6

n	α	β	γ	μ	δ	c_4
1	31.15	2.34	0	0	0	0
2	29.79	1.62	0	0.78	0	0
3	28.82	−0.14	0.57	0.82	0	0
4	30.69	0.97	0.20	0.78	2.97	0
5	28.57	0.30	0.38	0.69	0	0.001 30

$$D(\mathbf{0})=D_+ +D_- ,$$
$$D(\tau_1)=D_+ -D_- . \tag{37}$$

D_- is equivalent to a quadrupole interaction at large distances as before while D_+ leads to the well known LO-TO splitting of the optical modes.[13] This results from the conditional convergence of the dipole sum.

The quadrupole constants $Q(\tau)$ obey the symmetry relation $Q(\mathbf{0})=Q(\tau)$ in the diamond lattice. In the zinc-blende lattice we may write

$$Q(\mathbf{0})=Q_+ +Q_- ,$$
$$Q(\tau)=Q_+ -Q_- . \tag{37a}$$

B. LO-TO splitting

The LO-TO splitting[13] comes entirely from the term $\mathbf{K}=\mathbf{0}$ in Eq. (35) for $m=2$ (m is the order of differentiation) in the limit $k\to 0$, namely

$$\sum_{\mathbf{a}_l'} F^2_{q,ij}(\mathbf{a}_l+\mathbf{r})e^{i\mathbf{k}\cdot\mathbf{a}_l}=-\frac{N}{\text{vol}}\frac{4\pi}{k^2}k_i k_j+\text{analytic }(\mathbf{k}) . \tag{38}$$

Equation (38) then gives a nonanalytic contribution to the dynamic matrix from E^{2*}, namely

$$E^{2*}_{\text{NA}}=\sum_{\substack{i,j\\ \mathbf{t}_a\mathbf{t}_b=0,\tau_1}}\frac{N}{\text{vol}}\frac{8\pi}{k^2}k_i k_j M_i^1(\mathbf{t}_a)[M_j^1(\mathbf{t}_b)]^* ,$$
$$\text{in the limit } k\to 0 . \tag{39}$$

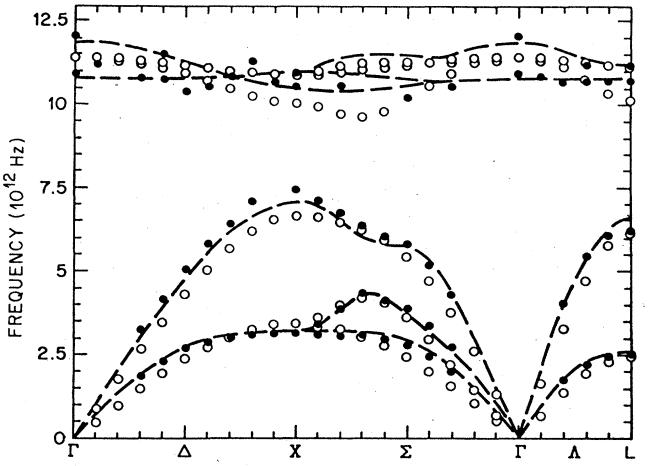

FIG. 6. Phonon dispersion curves for gallium phosphide. Open circles and dashes correspond to fits δ_1 and δ_4 in Table V. Solid circles are experimental data from Ref. 20.

In the limit $k\to 0$ we have the following expressions for the dipole moments:

$$M_i^1(\mathbf{t})=M_i^0 r_i(\mathbf{t}) \quad \text{(Kellermann)} ,$$
$$M_i^1(\mathbf{t})=D^s(\mathbf{t})\tfrac{4}{3}[r_i(\tau_1)-r_i(0)]/\tau \quad \text{(bond stretch)} , \tag{40}$$
$$M_i^1(\mathbf{t})=D^0(\mathbf{t})\tfrac{8}{3}[r_i(\tau_1)-r_i(0)]/\tau \quad \text{(bond tilt)} .$$

TABLE V. Gallium phosphide. See Table I.

$\mathbf{k}$ (units of $2\pi/a_L$)	ν (10^{12} Hz)	Weight	δ_1	δ_2	δ_3	δ_4
(0.4,0,0)	2.40	20	0.42*	0.50*	−0.01	0.01
	4.24	1	0.69	0.71	0.29	0.27
	10.83	2	−0.48	−0.31	−0.18	0.07
	11.61	1	0.47	−0.06	0.67	0.16
(1,0,0)	3.23	20	−0.26	−0.30	0.04	0.02
	7.51	1	0.80	0.81	0.38	0.43*
	10.60	2	−0.34	−0.25	−0.50	−0.40
	11.01	1	0.94	0.95	0.67	0.51
(0.5,0.5,0.5)	2.58	20	0.10	0.15	−0.01	0.01
	6.31	1	0.06	−0.46	0.03	−0.27
	10.78	2	−0.43	−0.27	−0.25	−0.03
	11.24	1	1.06	0.81	0.54	0.06
(0,0.6,0.6)	3.04	20	0.21	0.25	−0.07	−0.06
	4.19	2	0.09	−0.34	−0.12	−0.03
	6.13	2	0.17	0.17	0.75*	0.33
Max % error			18	21	12	6

n	α	β_1	β_2	γ_1	γ_2	μ	c_2
1	41.18	5.10	5.10	0	0	0	0
2	40.53	5.11	5.11	0	0	0	0.0121
3	32.54	35.32	−25.86	3.06	−1.72	1.14	0
4	31.03	35.03	−25.75	3.25	−1.71	1.21	0.0121

The right-hand side of Eq. (39) is zero for $\mathbf{r}$ perpendicular to $\mathbf{k}$. For $\mathbf{r}=r_L$ parallel to $\mathbf{k}$ we use Eq. (2) and Eq. (39) to obtain the nonanalytic contribution to the dynamical matrix. The analytic contribution is the same for both LO and TO modes. We then obtain the splittings

$$\omega_{\mathrm{LO}}^2-\omega_{\mathrm{TO}}^2=\frac{8\pi N}{\mathrm{vol}}C^2\left[\frac{1}{M_A(0)}+\frac{1}{M_A(\tau)}\right],$$
$$C=M_0^0 \text{ (Kellermann)},$$
$$C=\tfrac{8}{3}D_+^s/\tau \text{ (bond stretch)}, \quad (41)$$
$$C=\tfrac{16}{3}D_+^0/\tau \text{ (bond tilt)}.$$

We treat C as an empirical constant which is taken to satisfy Eq. (41) for the experimental values of $\omega_{\mathrm{LO}},\omega_{\mathrm{TO}}$.

IV. EMPIRICAL PARAMETER FITTING

We have tested the theory developed here by making an empirical fit to the phonon spectra of the diamond lattice materials C, Si, Ge, and Sn. We have also fit the zinc-blende compounds GaP, GaAs, and ZnS.

The fit was done by a weighted least-squares method using iterated linear extrapolation of the phonon matrices with respect to the interaction parameters. Approximately 20 separate phonons were fit. The $\mathbf{k}$ vectors, weights, frequencies, and errors of the fits together with the values of the fitting parameters are given in Tables I–VII.

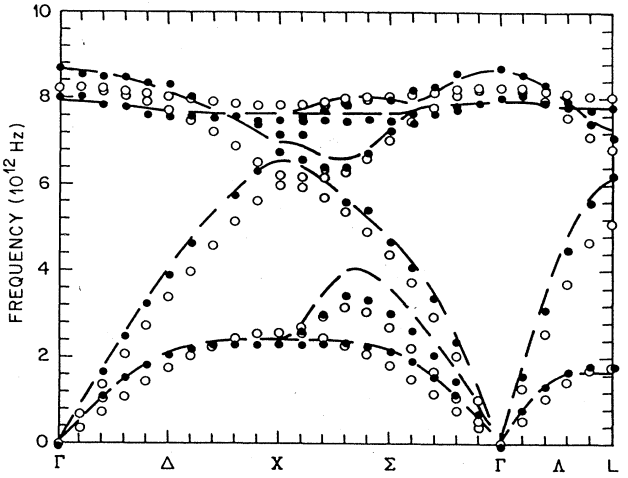

FIG. 7. Phonon dispersion curves for gallium arsenide. Open circles and dashes correspond to fits δ_1 and δ_4 in Table VI. Solid circles are experimental data from Ref. 21.

We have assumed that the phonon potential energy could be written in the form

$$U=\alpha U_\alpha+\beta_0U_{\beta0}+\beta_1U_{\beta1}+\gamma_0U_{\gamma0}+\gamma_1U_{\gamma1}+\delta_0U_{\delta0}+\delta_1U_{\delta1}+\mu U_M+E_q^2(+,f)+E_q^4(+,f), \quad (42)$$

The first eight interactions are defined by Eqs. (3), (8),

TABLE VI. Gallium arsenide. See Table I.

$\mathbf{k}$ (units of $2\pi/a_L$)	ν (10^{12} Hz)	Weight	δ_1	δ_2	δ_3	δ_4
(0.4,0,0)	1.88	10	0.40*	0.48*	−0.06	0.03
	3.30	1	0.52	0.54	−0.07	−0.04
	7.66	2	−0.49	−0.38	−0.19	−0.08
	8.42	1	0.47	0.11	0.44	0.11
(1,0,0)	2.36	10	−0.24	−0.26	−0.01	−0.05
	6.80	1	0.78	0.77	0.16	0.25
	7.22	1	0.97	0.97	0.29	0.26
	7.56	2	−0.30	−0.25	−0.07	−0.07
(0.5,0.5,0.5)	1.86	10	0.02	0.07	0.17	0.21
	6.26	1	1.12	0.54	0.59	0.13
	7.15	1	0.28	0.31	−0.08	−0.12
	7.84	2	−0.23	−0.14	−0.04	0.05
(0,0.7,0.7)	2.38	10	0.06	0.10	−0.06	−0.01
	3.48	2	0.30	0.01	−0.34	−0.52*
	5.65	2	0.26	0.25	−0.02	−0.03
	6.44	1	0.12	0.14	−0.12	−0.14
Max % error			21	25	10	15

n	α	β_1	β_2	γ_1	γ_2	μ	c_2
1	36.54	4.02	4.02	0	0	0	
2	36.18	3.96	3.96	0	0	0	0.0099
3	30.39	3.43	−4.61	2.04	0.65	1.76	0
4	30.53	2.52	−3.67	2.04	0.65	1.56	0.0099

TABLE VII. Zinc sulfide. See Table I.

k (Units of $2\pi/a_L$)	ν (10^{12} Hz)	Weight	δ_1	δ_2	δ_3	δ_4
(0.4,0,0)	2.05	20	0.37*	0.85*	−0.06	0.03
	3.57	1	0.47	0.64	−0.01	−0.03
	8.63	2	−1.12	−0.55	−0.30	−0.02
	10.31	1	0.73	−0.13	1.35	0.11
(1,0,0)	2.69	20	−0.27	0.05	0.09	0.02
	6.34	1	0.38	0.59	0.36	0.13
	9.47	2	0.03	0.35	−0.16	0.05
	9.90	1	1.39	1.69	0.45	0.64*
(0.5,0.5,0,5)	2.10	20	0.001	0.44	−0.13	−0.03
	5.85	1	0.36	−0.45	0.61	−0.27
	8.67	2	−1.00	−0.48	−0.43	−0.17
	10.10	1	1.43	1.08	0.25	−0.28
(0,0.6,0.6)	2.53	20	0.13	0.60	−0.06	−0.01
	3.56	20	0.07	−0.43	−0.01	−0.003
	5.50	2	0.23	0.38	0.87*	0.02
	10.06	1	0.34	0.61	−0.11	−0.14
Max % error			18	41	16	6

n	α	β_1	β_2	γ_1	γ_2	μ	c_2
1	30.95	3.54	3.54	0	0	0	0
2	29.17	2.56	2.56	0	0	0	0.0224
3	21.61	24.76	−20.97	3.42	−1.11	0.62	0
4	20.72	26.45	−22.30	3.27	−1.11	0.80	0.0224

(11), (14), and (16), respectively. The long-range Coulomb interactions E^2 and E^4 are defined in Eqs. (24a) involving dipole and quadrupole moments, respectively. The dipole and quadrupole moments are given by Eqs. (30) and (32).

We treat the dipole and quadrupole moments as constants to be determined empirically. We make the definition

$$E_{\mathbf{k}}^2(+,f)=c_2\eta_2(\mathbf{k}),E_{\mathbf{k}}^4(+,f)=c_4\eta_4(\mathbf{k})\,,$$
$$c_2=(D_+^0)^2/a_L^3\tau^2,\quad c_4=(Q_+^0)^2/a_L^5\tau^2\,, \tag{43}$$
$$\tau=\sqrt{3}a_L/4\,,$$

where η_2,η_4 are $\mathbf{k}$-dependent matrix forms yielding the dynamical matrix of Eq. (2). With these definitions $c_2,c_4,\alpha,\beta,\ldots$ have the same units which we take to be J/m^2 or 10^3 ergs/cm^2 in accord with Martin's convention.

The lattice sums are performed entirely in $\mathbf{k}$ space using Eq. (35). We have ignored the term F_ρ in Eq. (33) so that the Coulomb interaction $1/r$ has been replaced by the smeared interaction $(1/r)\mathrm{erf}(fr)$. This was done to improve the fitting. The quality of fit had a broad maximum around $f=3/a_L$ where a_L is the lattice constant. The same value of f was used for all materials and for both dipole-dipole and quadrupole-quadrupole interactions. The bond-tilt model was found to give a better fit than the bond-stretch model. An "equivalent quadrupole" model for the diamond lattice using $E_{\mathbf{k}}^2$ with $D^0(\mathbf{0})=-D^0(\tau_1)$ was tested but found to be not as good as the $E_{\mathbf{k}}^4(+,f)$ model finally adopted. The "Kellermann" model for $E_{\mathbf{k}}^2$ was found not to be as good as the bond-tilt model. The above conclusions were deduced from a study of several materials but were not thoroughly established.

In zinc-blende materials the parameter c_2 was fit to give the LO-TO splitting at $k=0$ exactly using Eq. (41). c_4 was set $=0$. In diamond lattices $c_2=0$ by symmetry

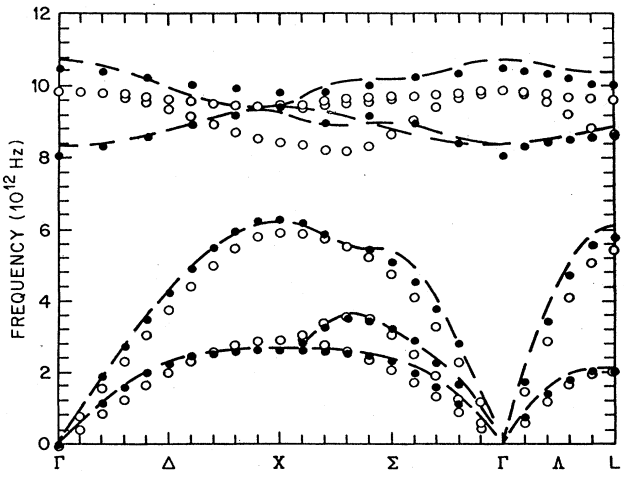

FIG. 8. Phonon dispersion curves for zinc sulfide. Open circles and dashes correspond to fits δ_1 and δ_4 in Table VII. Solid circles are experimental data from Ref. 22.

and c_4 was varied. Since c_4 is implicitly a square it must be positive to be meaningful. This was found to be true in all cases except diamond where the improvement in the fit from c_4 was negligible in any case.

The detailed fits are given in Tables I—VII and Figs. 2—8. The two-parameter Keating model gives a surprisingly good fit, even for the zinc-blende materials. The bond-bending parameter (β) we find is distinctly different from Martin's value which was determined by fitting the elastic constants. His value gives TA phonons which are much too high at the zone edges. For modeling short-range disturbances such as the displacements around an impurity our values are preferable since a Fourier analysis of the disturbance would find most of the weight at large **k** values.

Surprisingly, the addition of the constant c_2 to the Keating model which gives the correct LO-TO splitting does not improve the fit. For the less ionic material GaAs (Table VI) the fit is not improved by c_2 even for the six-parameter model. For GaP and ZnS (Tables V and VII) the addition of c_2 to the six-parameter model improves the fit considerably. (We are not counting c_2 as a "fitting parameter" because it is determined uniquely by the LO-TO splitting at $k=0$ and not by the least-square fit.)

Another unexpected result was the values of the bond-bending parameters β_1 and β_2 in the zinc-blende lattice. Although the Keating model with $\beta_1=\beta_2$ gives a reasonably good fit, the relaxation of the requirement $\beta_1=\beta_2$ gives hardly any further improvement. Also the values usually have opposite signs and are very much larger. This result suggests that the localization implied by the intuitively appealing picture of "bond bending" is not really true. We have a further theoretical objection to the bond-bending model. The Pauling hybrids on a given atom have no freedom to "bend" since they constitute a complete set which may most conveniently be described as a rigid tetrahedron. A better picture would seem to be a set of rigid tetrahedra on each atom which would be free to rotate relative to each other. This was the idea that motivated this investigation. The model is relatively awkward to implement, however, and did not produce better results than the Keating model so it was abandoned.

Another curious fact is that the more ionic compounds (GaP and ZnS) are fit better than GaAs although the model produces a good fit to the diamond-lattice compounds C, Si, Ge, and Sn.

In the diamond lattice we find that the order of importance of the parameters is $\alpha,\beta,\mu,\gamma,c_4,\delta$, except in diamond where the order of γ and μ is reversed. γ and μ are of nearly equal importance. In diamond c_4 is nonphysical (negative).

It is difficult to compare the quality of our fits to Weber's without using the same fitting procedure. In general it appears that our best fits (five parameter) are comparable to Weber's who also needed five parameters in diamond. Our five-parameter model appears to be less accurate but has the practical advantage of not using long-range (Coulomb) interactions. Our treatment features the importance of the McMurry *et al.* interaction shown in Fig. 1. The physical importance of the coplanar atom chains is emphasized by this result. The unusual spreading of the screening charge[8] along this direction is another result that points to the physical importance of the chains.

ACKNOWLEDGEMENTS

The author thanks W. Weber for helpful discussions.

[1]W. Weber, Phys. Rev. B **15**, 4789 (1977).
[2]H. Bilz and W. Kress, *Phonon Dispersion Relations in Insulators* (Springer, New York, 1979).
[3]M. T. Yin and M. L. Cohen, Phys. Rev. B **26**, 3259 (1982); **26**, 5668 (1982); K. Kunc and R. M. Martin, Phys. Rev. Lett. **48**, 406 (1982).
[4]G. A. Baraff, E. O. Kane, and M. Schlüter, Phys. Rev. B **21**, 5662 (1980).
[5]M. Lax, Phys. Rev. Lett. **1**, 133 (1958).
[6]R. M. Martin, Phys. Rev. **186**, 871 (1969).
[7]H. L. McMurry, A. W. Solbrig, Jr., J. K. Boyter, and C. Noble, J. Phys. Chem. Solids **28**, 2359 (1967); A. W. Solbrig, Jr., *ibid.* **32**, 1761 (1971).
[8]E. O. Kane, Phys. Rev. B **31**, 5199 (1985).
[9]R. M. Martin, Phys. Rev. B **1**, 4005 (1970).
[10]A. A. Maradudin, E. W. Montroll, and G. H. Weiss, *Solid State Physics,* Suppl. 3 (Academic, New York, 1963).
[11]P. N. Keating, Phys. Rev. **145**, 637 (1966).
[12]E. W. Kellermann, Phil. Trans. R. Soc. London, Ser. A **238**, 513 (1940).
[13]C. Kittel, *Introduction to Solid State Physics,* 4th ed. (Wiley, New York, 1971), p. 184.
[14]J. L. Warren, J. L. Yarnell, G. Dolling, and R. A. Cowley, Phys. Rev. **158**, 805 (1967).
[15]G. Dolling, *Inelastic Scattering of Neutrons in Solids and Liquids* (IAEA, Vienna, 1963), Vol. I, p. 37.
[16]G. Nilsson and G. Nelin, Phys. Rev. B **6**, 3777 (1972).
[17]G. Nilsson and G. Nelin, Phys. Rev. B **3**, 364 (1971).
[18]G. Nelin and G. Nilsson, Phys. Rev. B **5**, 3151 (1972).
[19]D. L. Price, J. M. Rowe, and R. M. Nicklow, Phys. Rev. B **3**, 1268 (1971).
[20]J. L. Yarnell, J. L. Warren, R. G. Wenzel, and P. J. Dean, *Neutron Inelastic Scattering* (IAEA, Vienna, 1968), Vol. 1, p. 301.
[21]J. L. T. Waugh and G. Dolling, Phys. Rev. **132**, 2410 (1963).
[22]N. Vagelatos, D. Wehe, and J. S. King, J. Chem. Phys. **60**, 3613 (1974).